Transactions on Energy Systems and Engineering Applications

Article

A battery energy storage system as an alternative for mitigating issues in the distribution network

Thiago Luiz Caretta[1], Vitor Teles Correia[1,*], John Jefferson Antunes Saldanha[1] and Rodrigo Trentini[1]

[1] Department of Electrical Engineering, Federal Institute of Santa Catarina, Jaraguá do Sul, Brazil.
[*] Correspondence: vitor.correia@ifsc.edu.br

Received: 30 October 2023; Accepted: 21 March 2024; Published: 31 July 2024

Abstract: This study explores the application of a Battery Energy Storage System (BESS) within a distribution network to boost energy efficacy. The investigation specifically scrutinizes the integration of BESS into the distribution network feeder, both in the presence and absence of distributed photovoltaic penetration, with a focus on enhancing load factor and power factor. Utilizing the OpenDSS software with a Python interface, simulations were conducted to assess a range of scenarios involving the injection and absorption of active and reactive power. The outcomes underscore noteworthy enhancements in both load factor and power factor at the feeder output. Additionally, the integration of BESS exhibits a reduction in power losses along the feeder. These findings offer valuable perspectives for advancing energy efficiency in distribution networks, and have implications for future research and practical implementation.

 https://doi.org/10.32397/tesea.vol5.n2.575

1. Introduction

The quest for enhanced energy efficiency in electric power distribution systems has intensified, driven by the escalating electricity demand and mounting environmental concerns [1,2]. Amidst various technologies gaining traction in distribution networks globally, Battery Energy Storage Systems (BESS) have emerged as a promising solution [3]. These systems offer diverse applications within the power sector, facilitating improved control over power factors and demand curve shaping, thereby curbing peaks and easing strain on transmission and distribution systems. Furthermore, the strategic deployment of BESS can effectively redistribute demand across the day, enhancing the system's load factor, thereby relieving grid load and deferring investments in infrastructure.

Furthermore, BESS can effectively address challenges posed by distributed generation. They can be directly manipulated by system operators, mitigating issues related to intermittency and the low capacity factor of renewable sources like solar and wind. Given the variability of these sources, BESSs can be instrumental in efficiently harnessing renewable energy and ensuring operational flexibility, thereby

How to cite this article: Caretta, Thiago Luiz; Correia, Vitor Teles; Saldanha, John Jefferson Antunes; Trentini, Rodrigo. A battery energy storage system as an alternative for mitigating issues in the distribution network. *Transactions on Energy Systems and Engineering Applications*, 5(2): 575, 2024. DOI:10.32397/tesea.vol5.n2.575

contributing to maintaining a consistent power supply and enhancing its quality [4]. Notably, among various battery technologies, lithium-ion batteries hold a prominent position in BESSs [5], thus serving as the focal point of this study.

Lithium-ion batteries represent cutting-edge technologies extensively employed in electronic devices, electric vehicles, and energy storage systems. Renowned for their high energy density, prolonged lifespan, and consistent performance, these batteries undergo assessment based on several parameters, including maximum depth of discharge (DoD), state of charge (SoC), number of cycles, and operating temperature. As per [6], lithium batteries typically offer a cycle life of 500 to 600 times, but this value can reach 1000 cycles or more, contingent upon the DoD. Furthermore, operating temperature significantly influences battery lifespan, with optimal performance achieved at room temperature, as heightened temperatures accelerate ageing by amplifying internal resistance [7].

Numerous studies have been dedicated to exploring the potential of BESS in distribution networks. Some have concentrated on optimising storage system sizes for voltage regulation and peak load reduction [8], while others have evaluated electric network performance with BESS through simulations [9–11]. In addition, [12] have applied battery energy storage for frequency regulation and peak shaving. Moreover, [13] proposed the adoption of a battery system to mitigate adverse impacts caused by high penetration of solar power. Furthermore, [14] studied the utility-scale BESS's utilisation to assist grid operators in managing congestion and active power imbalance. Consequently, the integration of BESS in distribution networks has exhibited favourable outcomes, such as load curve smoothing and improved load factors. Nonetheless, it remains imperative to assess the impacts and potential drawbacks of BESS integration in actual distribution networks.

This study aims to scrutinise the implications of integrating a BESS into a real distribution network feeder in Jaraguá do Sul, Brazil. The objectives encompass enhancing the load factor, power factor, and identifying other consequential effects, both positive and negative. The study entails defining BESS specifications, modelling it using OpenDSS software, and conducting simulations with diverse scenarios. The analysis will primarily emphasise the achieved enhancements in load factor and power factor, as well as the potential benefits and areas for enhancement arising from BESS integration.

It is important to note that certain aspects of the distribution system lie beyond the scope of this paper, such as the load growth rate, peak load duration, potential economic improvements during off-peak periods, and the utilisation of the proposed solution as an ancillary service.

This paper's structure is as follows: Section 2 outlines the methodology, detailing the feeder, BESS modelling, and simulation scenarios. Section 3 presents the study's results, with a specific focus on the penetration of photovoltaic generation in conjunction with BESS utilisation. Finally, Section 4 offers conclusions and suggestions for future research endeavours.

2. Methodology

2.1. Feeder JSL07

The JSL07 distribution feeder, originating from the JSL substation in Jaraguá do Sul, Santa Catarina, Brazil, serves as the focal point of this investigation. The modelling data utilised stems from the Distribution System Operator's 4th Periodic Tariff Review conducted in 2016 [15]. Selection of this specific feeder was informed by its use in other scholarly works [16, 17], allowing for comprehensive comparisons among studies and diverse real-world implementations. It is worth noting that, based on the available data, the JSL07 feeder is devoid of voltage regulators, distributed generation (DG), and reactive power compensator units. Additionally, the feeder caters to approximately 620 consumer units, with 98% falling under the low voltage category and the remaining 2% under medium voltage. Moreover, it encompasses 24 distribution transformer units, with detailed specifications provided in Table 1.

Table 1. Characteristics of feeder JSL07 [18].

Description	Quantity
Medium voltage segments	148
Low voltage segments	171
Distribution transformer units	24
Medium voltage transformer units	13
Low voltage transformer units	604

In a prior study [16], various penetration levels of photovoltaic distributed generation (PVDG) were investigated within the feeder. For this research, in addition to the scenario without PVDG, a 25% penetration of PVDG has been incorporated. This 25% corresponds to the aggregate installed power of photovoltaic generators across the consumer units (UCs), amounting to a quarter of the nominal power of the distribution transformer to which the PVDG loads are linked. Each PVDG unit has an installed capacity of 8.5 kW.

Analysing the modelled data, both with and without PVDG, provides insights into the active and reactive power demands originating from the substation via the JSL07 circuit over weekdays throughout the day, as illustrated in Figure 1. As PVDG solely injects active power, the reactive power curves are superimposed for comparison.

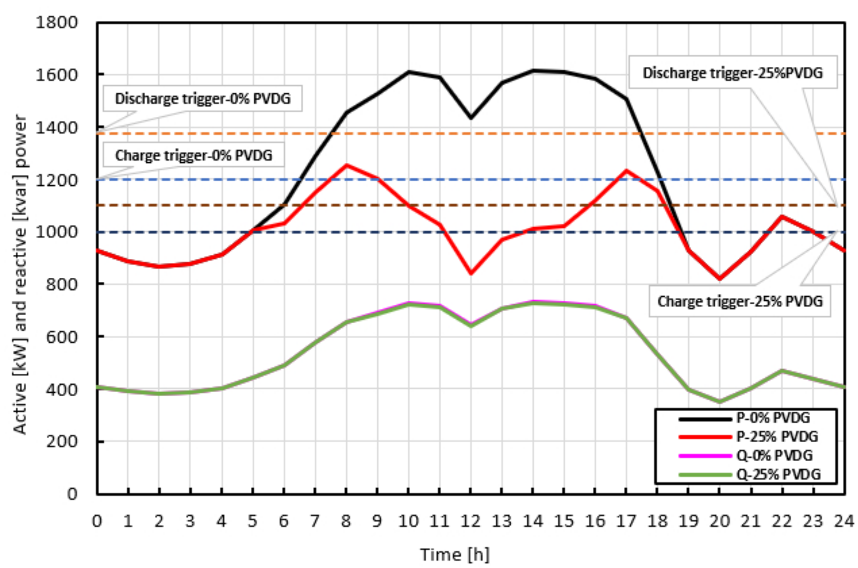

Figure 1. Power demanded by the feeder with 0% and 25% of PVDG and their respective charge and discharge triggers.

2.2. OpenDSS tools

The Open Distribution System Simulator (OpenDSS) is a powerful software developed by the Electric Power Research Institute (EPRI) for simulating distribution systems, including the integration of Distributed Generation (DG) and Energy Storage Systems (ESS). It enables power flow studies, technical loss analysis, and harmonic distortion studies [19]. OpenDSS is an open-source software that supports the development of Smart Grids and allows users to create their own DLL to address specific study challenges [19].

The py-dss-Interface in conjunction with PyCharm provides an integrated development environment for controlling OpenDSS using Python. It offers various features that facilitate OpenDSS development through Python programming, enabling simulations in different scenarios without modifying the initial code. Python-controlled OpenDSS simulations support loops, filtering conditions, and other functionalities provided by the Python language.

The Storage element in OpenDSS simulates an ESS in the electrical network. It can operate autonomously or be controlled by the StorageController and/or InvControl elements. The Storage element incorporates various temporal variations, such as daily, annual, or DutyCycle modes [20]. It includes components like ideal storage, charge and discharge losses, state of charge, inverter, and idle period losses [20].

The StorageController element allows for the simultaneous control of multiple energy storage units, providing intelligent charging and discharging modes [21]. It offers various charging modes, including PeakShaveLow and I-PeakShaveLow, as well as several discharging modes such as PeakShave, I-PeakShave, Follow, Support, and Schedule [21].

These features make OpenDSS a valuable tool for simulating distribution systems and studying the integration of energy storage systems. The software capabilities and flexibility enable researchers to analyse various scenarios and investigate the impact of different control strategies on system performance and energy efficiency, therefore it is the selected software for the simulations and analysis in this work, as is shown in the next section.

2.3. Modeling of the BESS

The modelling of the BESS is conducted utilising Python software version 3.7.9, with the support of the PyCharm development environment version 2022.3.3 and the py-dss-interface package version 1.0.2. These operate in conjunction with OpenDSS version 9.4.2.2 (64-bit build). Python through PyCharm was preferred due to its versatile simulation capabilities and potential for implementing optimisations and programming routines in future research endeavours.

In the BESS model, the Storage element is defined by several essential parameters, including the number of phases, bus connection, nominal voltage, reactive power (kvar), power factor (pf), apparent power rating, efficiency curve, active power output, energy storage capacity, current energy stored, and idle losses [20].

It is pertinent to mention that the kvar and pf parameters are mutually exclusive. Additionally, in the specific version of OpenDSS employed, the DispMode parameter does not need to be defined as EXTERNAL, as the Storage element automatically assumes the EXTERNAL mode upon the addition of the StorageController.

Complementing the model, the StorageController element defines parameters such as the element to be monitored (e.g., line or transformer), terminal number, number of monitored phases, BESS discharge and charge triggers, operation modes, and reserve capacity percentage [21].

Regarding the BESS modelling, several parameters, including kWrated, kWhrated, kvar, and %stored, necessitate calculation. The kWrated parameter is determined as the active power of the inverter, ensuring that it exceeds the calculated value of $P_{\text{nec}}(t)$, derived from the equation below:

$$P_{\text{nec}}(t) = P_{\max}(t) - \text{kWTarget}, \tag{1}$$

$$\text{kWrated} > P_{\text{nec}}(t). \tag{2}$$

where kWrated is greater than $P_{\text{nec}}(t)$.

The energy storage capacity (kWhrated) is ascertained considering losses, including inverter losses ($P^{ch}_{losses,inv}(t)$) and charging losses ($P^{ch}_{losses,ch}(t)$), expressed by the equations [20]:

$$P^{ch}_{losses,inv}(t) = P_{in}(t) \cdot (1 - \eta_{inv}(t)), \tag{3}$$

$$P^{ch}_{losses,ch}(t) = (P_{in}(t) \cdot \eta_{inv}(t) - P_{idl}) \cdot (1 - \eta_{ch}), \tag{4}$$

$$P^{ch}_{losses,tot}(t) = P^{ch}_{losses,inv}(t) + P_{idl} + P^{ch}_{losses,ch}(t), \tag{5}$$

$$P^{ch}_{eff}(t) = P_{in}(t) - P^{ch}_{losses,tot}(t). \tag{6}$$

Similarly, discharging losses ($P^{dch}_{losses,inv}(t)$ and $P^{dch}_{losses,dch}(t)$) are determined by the equations [20]:

$$P^{dch}_{losses,inv}(t) = P_{out}(t) \cdot \left(\frac{1}{\eta_{inv}(t)} - 1 \right), \tag{7}$$

$$P^{dch}_{losses,dch}(t) = \left(\frac{P_{out}(t)}{\eta_{inv}(t)} + P_{idl} \right) \cdot \left(\frac{1}{\eta_{dch}} - 1 \right), \tag{8}$$

$$P^{dch}_{losses,tot}(t) = P^{dch}_{losses,inv}(t) + P_{idl} + P^{dch}_{losses,dch}(t), \tag{9}$$

$$P^{dch}_{eff}(t) = P_{out}(t) + P^{dch}_{losses,tot}(t). \tag{10}$$

These equations consider the inverter efficiency ($\eta_{inv}(t)$), idle losses (P_{idl}), and discharge efficiency (η_{dch}).

The %stored parameter's definition involves simulating the insertion of the BESS over several days, commencing with a fully discharged state to attain steady-state conditions and determine the necessary stored energy for initialising the BESS. In this study, the %stored parameter was set to 55% for scenarios without PVDG and 61% for the 25% PVDG scenario.

Temperature variations are not considered in this model, and thus, the BESS operates at its nominal capacities. The substation output is the element monitored, while the inverter's apparent power is set at 530 kVA, aligning with the specifications of a real system [22]. The BESS is connected at the nearest medium-voltage bus to the substation.

2.4. Simulation Scenarios

The simulation scenarios were meticulously structured, encompassing two fundamental cases: one without PVDG and the other incorporating PVDG (C1a and C2a, respectively). Each of these cases was further subdivided to integrate the BESS with its diverse functionalities, including active and reactive power injection and absorption. The detailed breakdown of the scenarios and their corresponding subdivisions is as follows:

- Scenario 1a (C1a): Considers the situation with 0% PVDG penetration, operating without any intervention from the BESS.
- Scenario 1b (C1b): Assumes 0% PVDG penetration, with the BESS maintaining a steady unity power factor throughout its operations.
- Scenario 1c (C1c): Accounts for 0% PVDG penetration, with the BESS sustaining a consistent 0.92 lagging power factor through strategic active and reactive power adjustments.
- Scenario 1d (C1d): Explores the circumstance of 0% PVDG penetration, where the BESS is actively involved in the continuous injection of 300 kvar to address specific reactive power requirements.
- Scenario 2a (C2a): Focuses on a scenario with 25% PVDG penetration, without direct BESS intervention.

- Scenario 2b (C2b): Involves 25% PVDG penetration, with the BESS ensuring a constant unity power factor for optimised performance.
- Scenario 2c (C2c): Addresses the 25% PVDG penetration situation, with the BESS operating to maintain a steady 0.92 lagging power factor, effectively managing the system's power quality.
- Scenario 2d (C2d): Examines the impact of 25% PVDG penetration, with the BESS consistently injecting 300 kvar to mitigate potential power factor concerns and ensure grid stability.

In scenarios C1c and C2c, active and reactive power injection and absorption are coordinated to preserve the BESS power factor at 0.92 lagging, maintaining optimal operational conditions. On the other hand, scenarios C1d and C2d involve the strategic utilization of the BESS to address a portion of the system's reactive demand, thereby rectifying the substation's power factor to levels acceptable to the electricity utility.

The evaluation of results pertaining to Load Factor (LF) enhancement follows a comprehensive methodology outlined in [23]. This involves a meticulous comparison utilising the criterion: $LF_{\text{original}} < LF_{\text{corrected}} \leq 1$, where ($LF_{\text{original}}$) signifies the original load factor, and ($LF_{\text{corrected}}$) represents the corrected load factor following BESS integration. Moreover, the analysis of Power Factor (PF) entails a scrutiny of values lower than 0.92 lagging during the daytime period to ensure optimal power quality. Furthermore, the assessment encompasses a detailed analysis of both active and reactive system losses, providing valuable insights into the overall system efficiency and performance.

For completeness, Figure 2 demonstrates the layout of the JSL07 feeder, obtained through the OpenDSS software running through the Python interface. The green square shows the location of the substation, and the red circle represents the location of the BESS.

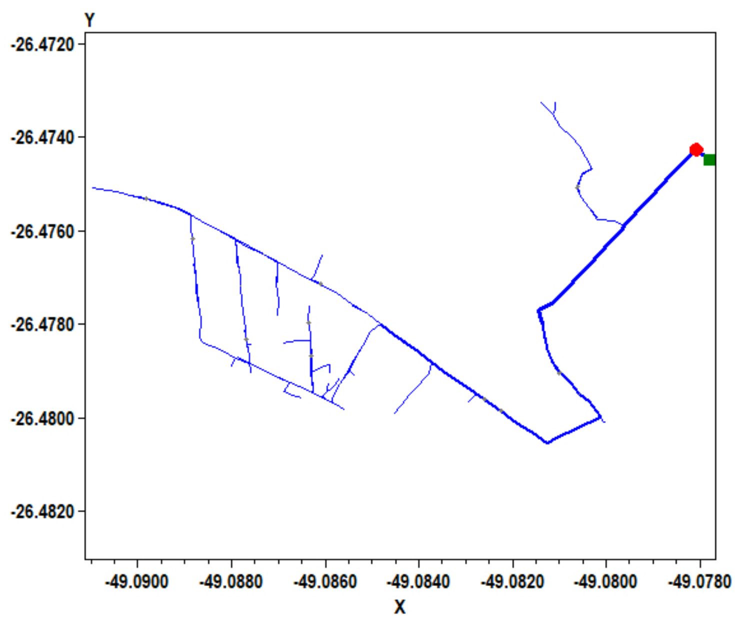

Figure 2. Layout of the JSL07 feeder.

3. Results

This section delves into the detailed analysis of BESS performance, comprehensively examining the intricate dynamics of power injection and absorption, electrical energy flow, Load Factor (LF), and Power Factor (PF) variations throughout the entire day across the different outlined scenarios. Moreover, a thorough assessment of losses along the distribution feeder, encompassing both active and reactive power components, is conducted to provide a holistic understanding of system efficiency.

Furthermore, this study closely investigates the synergistic impact of BESS along with PVDG within the distribution network, elucidating the combined contributions of these technologies in shaping the overall operational landscape. By evaluating the interplay between BESS and PVDG, this analysis aims to unveil the intricate relationship and potential benefits related to their integration within the distribution network framework.

3.1. BESS State in Diverse Scenarios

The BESS operates dynamically across a spectrum of scenarios, each presenting unique characteristics and behaviours. The state of the battery, power and energy fluctuations, LF, PF, and the interplay of BESS with PVDG are all subjects of detailed scrutiny.

Figure 3 vividly portrays the intricate electrical energy profile of the BESS as it navigates through the day across two pivotal scenarios: one with 0% PVDG penetration and the other with a 25% PVDG integration. Additionally, this figure offers insights into the battery's SoC over time, providing a visual representation of its continuous operation.

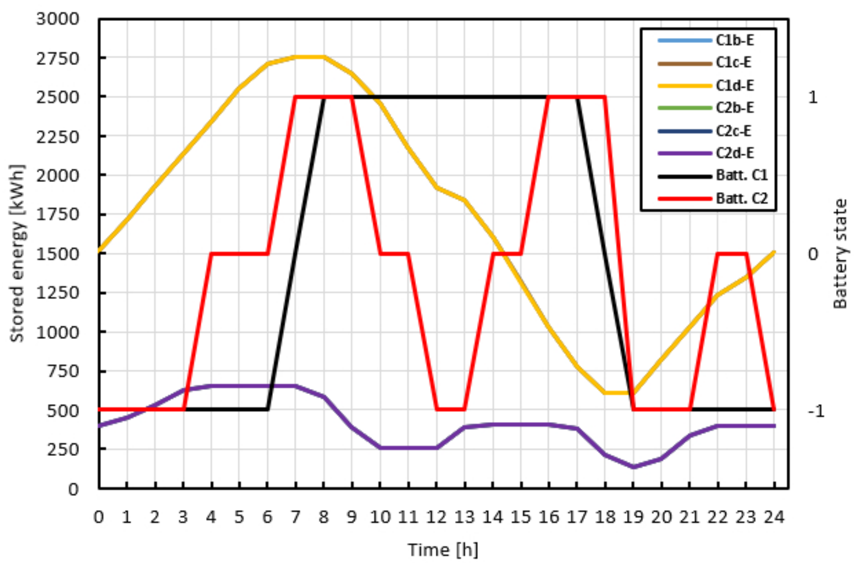

Figure 3. Energy dynamics and battery condition in scenarios with 0% and 25% PVDG, alongside BESS integration.

The examination of these curves reveals patterns shared by scenarios C1b, C1c, and C1d. It becomes evident that the BESS initiates charging when the curve approaches a value of -1 and discharges when it nears 1. The points hovering close to zero signify moments of idle state. Commencing with an initial energy of approximately 1,500 kWh, predicated on a 55% value for the %stored parameter, charging ensues until 7h, peaking at 2,750 kWh during idle periods. The discharge phase spans from 8h to 17h, with the battery returning to an idle state by 18h, maintaining an energy reserve of approximately 612 kWh. Charging recommences at 19h, perpetuating the cycle throughout the 24-hour cycle.

Figure 3 also charts the SoC of the BESS, which begins at 55% and descends to around 22% at the conclusion of the discharge and idle states. DoD approximates 78% by the discharge phase's culmination. The initial BESS energy calculation, involving a 29% reserve, aligns with the observed outcome, resulting in a 22% reserve. This discrepancy is attributed to ongoing discharging during the transition between discharge and idle states. However, this variation remains within the acceptable limit of a 20% reserve, equivalent to a maximum DoD of 80%.

Scenarios C2b, C2c, and C2d present analogous patterns. The BESS initiates operations with approximately 400 kWh (representing 61% of the stored parameter) and ascends to 650 kWh at 4h during idle phases. The day unfolds with alternating periods of discharge, idle states, and brief charging interludes, eventually culminating in an approximate energy level of 400 kWh by 21h, launching a new cycle. The SoC oscillates between 61% and 21%, while DoD spans a range from 39% to 79%. Despite a slight variance from the expected 20% reserve, the recorded energy reserve stands at 26%.

Moving to Figure 4, the representation of active and reactive power injection and absorption for the BESS within scenarios excluding PVDG unfolds. These scenarios share similar behaviours, with the BESS absorbing a maximum power of 250 kW during the early hours, gradually diminishing as it approaches full charge. Active power injection varies based on feeder demand and discharge triggers, never exceeding the 250 kW threshold. Active power injection occurs at 14h, approximating 24 kW. During the BESS's idle periods at 7h and 18h, neither active power injection nor absorption is observed. Reactive power displays variations contingent on the scenario: Scenario C1c seeks to sustain a power factor of 0.92 lagging, Scenario C1d maintains a constant injection of 300 kvar, while Scenario C1b operates solely with active power, resulting in negligible reactive power.

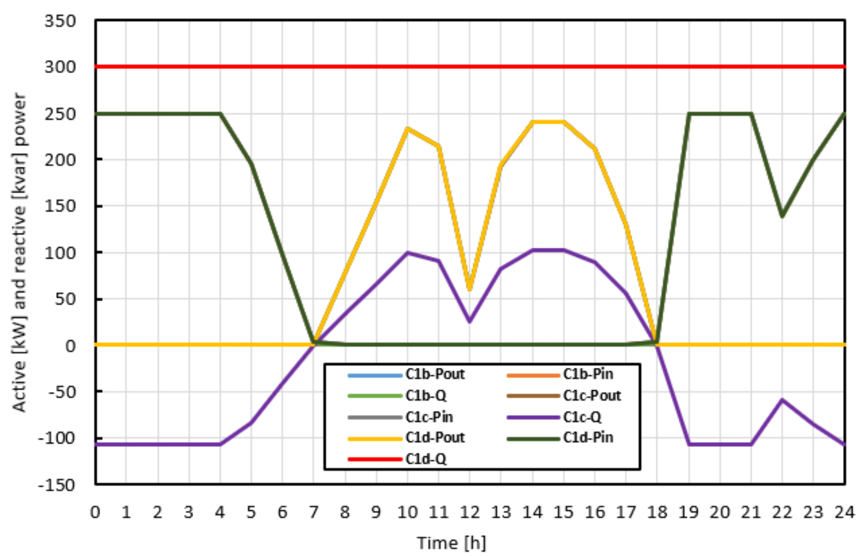

Figure 4. Active and reactive power injection and absorption in scenarios without PVDG, integrated with BESS.

The exploratory journey extends further into the dynamic landscape, as illustrated in Figure 5, which unveils the injection and absorption of active and reactive power in scenarios featuring 25% PVDG. The active power injection and absorption profiles mirror their counterparts in scenarios without PVDG, with maximum absorption observed in the early hours, while injection levels are determined by the differential between feeder demand and the discharge trigger. The reactive power trajectory diverges in accordance with the specific scenario: Scenario C2c strives to sustain a power factor of 0.92 lagging, Scenario C2d injects a constant 300 kvar, and Scenario C2b operates solely with active power.

In summary, this comprehensive analysis offers profound insights into the multifaceted performance of the BESS system across diverse scenarios. By examining critical parameters such as electrical energy, active and reactive power injection and absorption, SoC, DoD, and PF, this study provides valuable information

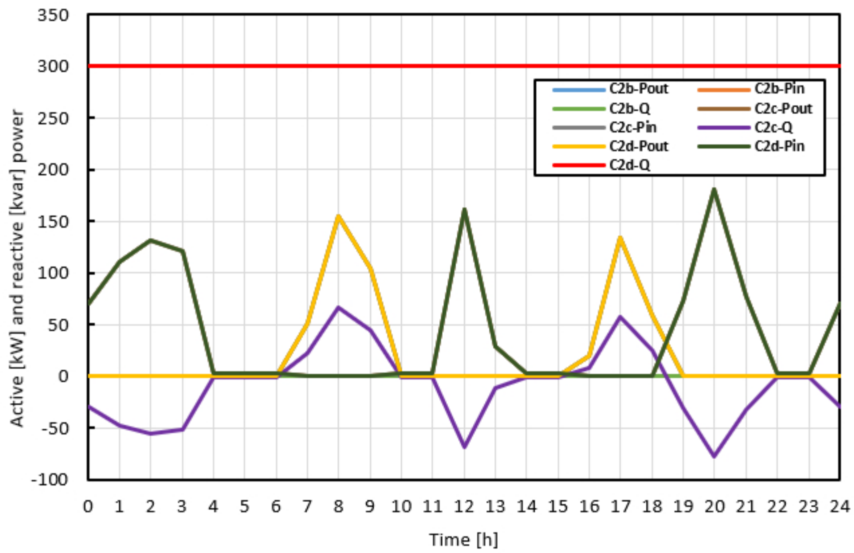

Figure 5. Active and reactive power injection and absorption in scenarios with 25% PVDG, integrated with BESS.

about the pivotal role played by BESS when seamlessly integrated with PVDG within the distribution network.

3.2. Feeder Load Factor

Figure 6 provides an insightful view of the feeder demand with and without the integration of a BESS for various load and discharge scenarios. The graph reveals that from 19h to 6h, the feeder demand experiences an increase as the BESS requires active power for charging. Between 8h and 17h, the demand curve remains relatively constant as the BESS injects active power, thereby mitigating the substation's power demand. This shift in consumption is a deliberate strategy aimed at enhancing the feeder's load factor.

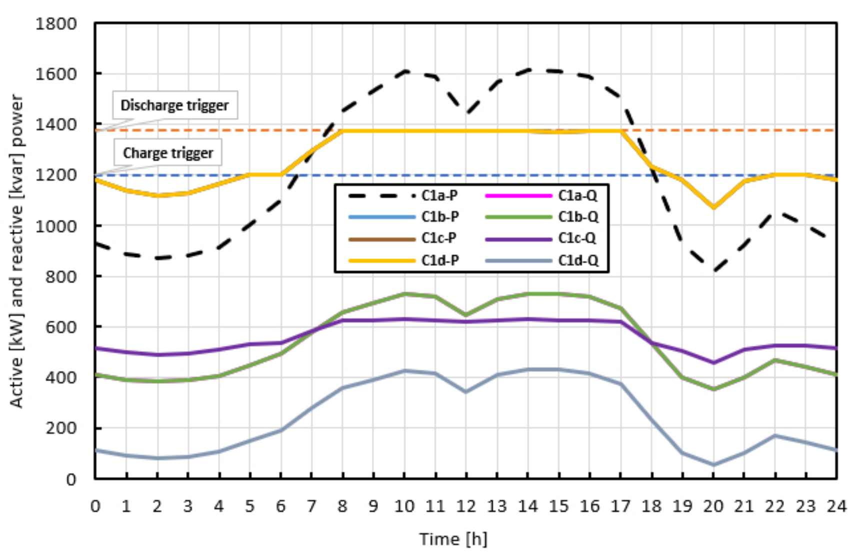

Figure 6. Power demanded by the feeder with 0% of PVDG and the integration of a BESS.

The active power absorption and injection are accordingly to the pre-defined triggers. During the charging phase, the feeder's demand occasionally drops below the charging trigger due to the power limit of 250 kW. Nevertheless, during the discharge phase, the adopted energy capacity effectively shapes the demand. The BESS's injection of reactive power throughout the day is also evident. In scenarios C1a and C1b, in which the BESS injects only active power, the reactive power demand from the substation overlaps. However, in other scenarios like C1c, the BESS regulates reactive power to maintain a power factor of 0.92 lagging, redistributing the reactive power demand to periods of lower utilisation. In C1d, the BESS's constant injection of 300 kvar of reactive power uniformly reduces the feeder's reactive power demand. The injection or absorption of reactive power has implications on the power factor, voltage levels, and losses along the feeder. The reshaping and flattening of the demand curve contribute to an improvement of approximately 21.05% in the load factor, reducing peak demand and enhancing the grid's efficiency.

Figure 7 portrays the feeder demand with 25% PVDG and the integration of the BESS. The demand curve adheres to the pre-defined triggers, strategically shifting consumption to periods of lower utilisation and optimising the demand curve during peak hours. The injection of reactive power by the BESS varies across scenarios, with scenario C2c maintaining a power factor of 0.92 lagging, and scenario C2d injecting a constant 300 kvar of reactive power. The incorporation of the BESS in scenarios with 25% PVDG results in a 16.05% improvement in the load factor, demonstrating heightened system efficiency and sustainability.

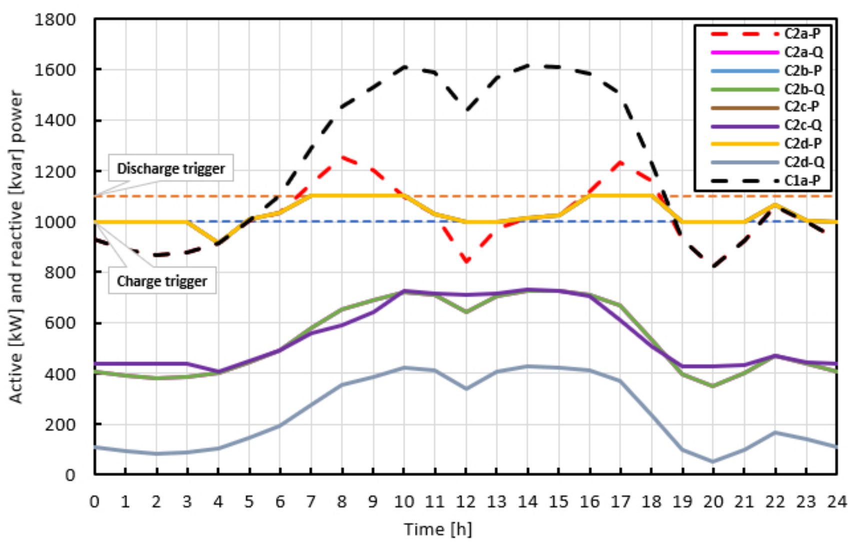

Figure 7. Power demanded by the feeder with 25% of PVDG and the integration of a BESS.

3.3. Feeder Power Factor

Figure 8 presents the PF at the substation output without PVDG for various scenarios throughout the day. In scenarios C1a and C1c, the PF slightly lags below 0.92. Scenario C1b exhibits fluctuations in PF during BESS charging and discharging, with a minimum PF of around 0.88 during certain daytime hours. In scenario C1d, the constant injection of 300 kvar significantly improves the PF during the daytime, with a minimum PF of approximately 0.95. Scenarios C2a and C2c display similar PF curves, while scenario C2b demonstrates PF fluctuations during BESS charging and discharging. The lowest PF is recorded at 14h, which scenarios C2b and C2c both exhibit a PF of 0.81. By incorporating a constant reactive power injection of 300 kvar in scenario C2d, the minimum PF improves to 0.92 at 14h. Enhanced power factor contributes to increased system efficiency, bolstering environmental sustainability, optimising equipment performance, and enhancing the overall reliability of the distribution network.

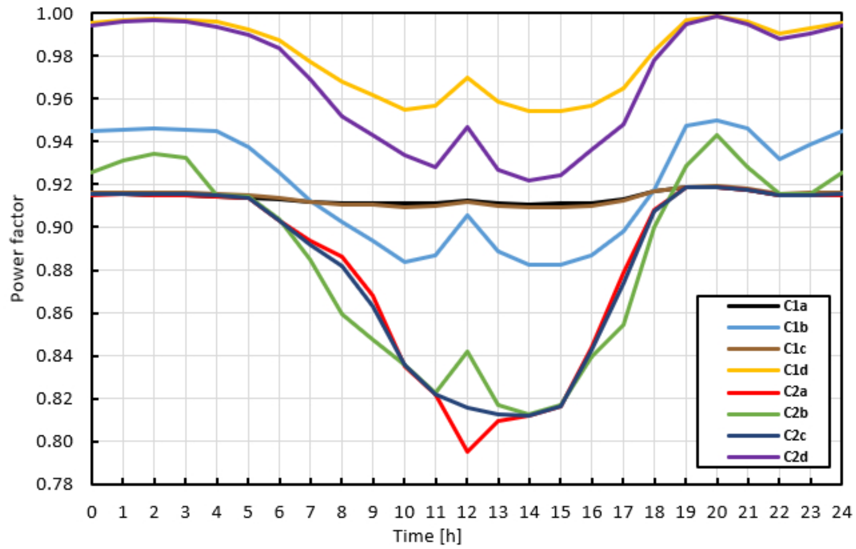

Figure 8. Power factor at the feeder output with 0% and 25% of PVDG and the integration of a BESS.

3.4. Voltage levels

The analysis of voltage levels at the low-voltage (LV) (Figure 9(a) and (b)) buses reveals important insights. In the simulations, the focus is on the 14h time frame, as it exhibited significant voltage elevations along the feeder. The LV buses are numbered from 1 to 146, corresponding to their identification codes in the Geographic Database of the Distributor (BDGD). Considering the initial scenarios without and with distributed photovoltaic generation (PVDG) (C1a and C2a) and scenarios C1d and C2d (which showed improvements in the feeder capacity factor and power factor), it is observed that no voltage violations occur in the LV buses for scenarios without PVDG. However, in scenarios with PVDG, approximately 5.48% of the monitored LV buses (eight buses) displayed violations.

Moving on to the medium-voltage (MV) buses (Figure 9(c) and (d)), the focus is also on the 14h time frame. The MV buses are numbered from 1 to 149. In the analysis, the same scenarios are considered: C1a, C2a, C1d, and C2d. It is observed that there are no voltage violations in the MV buses across all the presented scenarios. However, a slight increase in voltage levels is noticed in the MV buses due to the constant injection of reactive power from the BESS. It is important to note that the increase in voltage levels is primarily attributed to the installed photovoltaic systems, as there are no significant voltage elevations between C1a and C1d or between C2a and C2d.

To address the voltage elevations, potential solutions can be considered. Firstly, adjusting the tap settings of distribution transformers to 1 pu on the primary side, as the current OpenDSS model has them set at 0.9565 pu [18]. Another solution involves controlling the photovoltaic inverters to process reactive power at the LV buses [17]. Additionally, a detailed analysis of voltage regulators could be performed to monitor critical voltage levels and automate tap changes when voltage values approach the limits. These measures would contribute to maintaining safe voltage levels and ensure the proper operation of the distribution network.

3.5. Losses Analysis and Feeder Efficiency

The comprehensive evaluation of losses along the feeder provides crucial insights into the efficiency of the system under various scenarios. For the base scenarios C1a and C2a, minor reductions in losses were observed during specific hours, particularly during the discharge periods of the BESS. This reduction

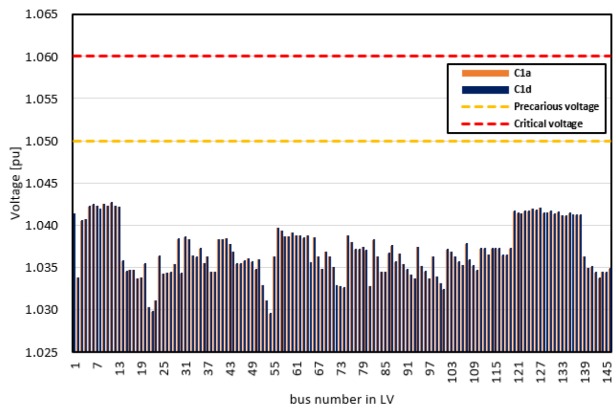

(a) Scenario C1a and C1d for LV

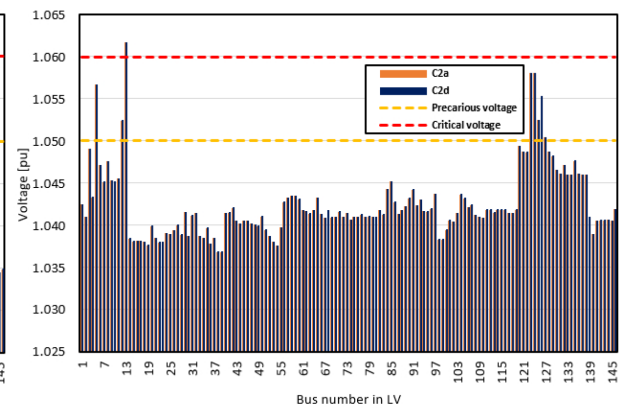

(b) Scenario C2a and C2d for LV

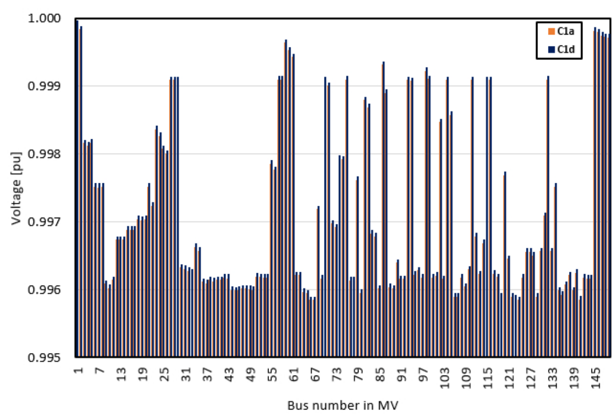

(c) Scenario C1a and C1d for MV

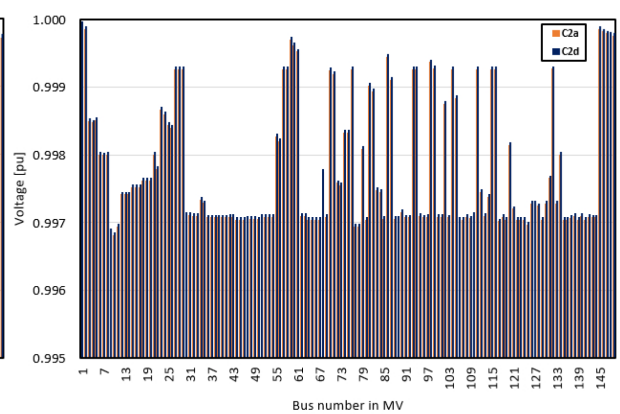

(d) Scenario C2a and C2d for MV

Figure 9. Low and Medium Voltage levels (LV and MV) for scenarios C1a, C1d, C2a and C2d.

can be attributed to the proximity of the BESS to the substation, which helped alleviate the feeder section between the substation and the BESS. Conversely, in scenarios involving PVDG, there was a marginal decrease in losses during the discharge periods, indicating the synergistic effects of the BESS and PVDG integration in enhancing feeder efficiency.

However, the placement of the BESS closer to the origin of the feeder limited the extent of improvement. If the BESS were positioned further downstream, it could potentially provide more significant relief to the feeder, leading to overall reduced losses during both charging and discharging periods. However, such a modification might introduce challenges, such as increased losses during charging, which would need to be carefully considered in the overall optimisation strategy.

3.6. BESS and PVDG Contributions in the Distribution Network

The analysis of the contributions from different devices in the distribution network is crucial for understanding the overall dynamics and power flow within the system. Figure 10 clearly illustrates the dynamic interactions between the PVDG and the BESS in terms of active power injection and absorption. The dominance of the PVDG in terms of power injection is evident, with negative values representing the injection of active power into the system. In contrast, the BESS exhibits a dual role, with positive values indicating active power absorption during charging and negative values indicating active power injection

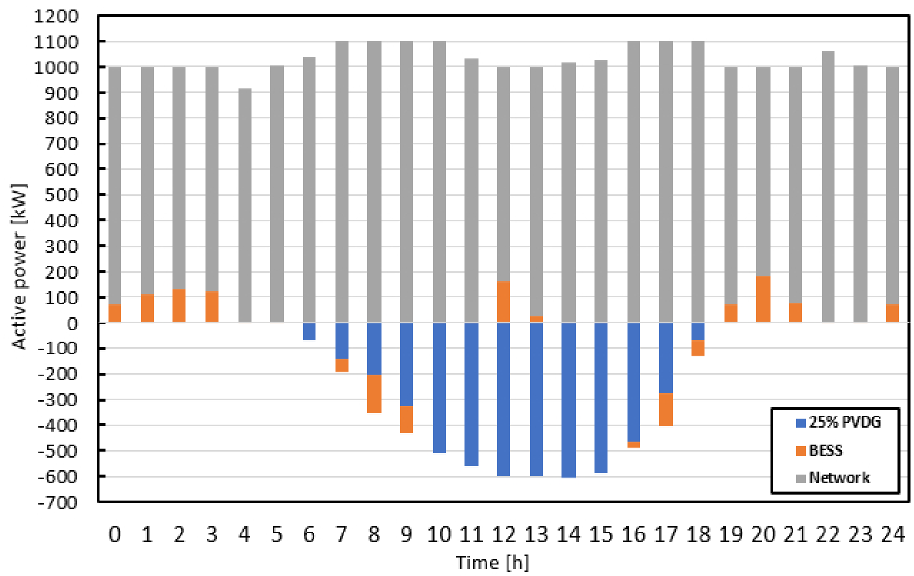

Figure 10. Contributions of the BESS and PVDG to the network active power.

during discharging, effectively regulating the overall power dynamics in the distribution network. This comprehensive understanding of the contributions of these key elements is vital for the effective design and implementation of future sustainable and efficient distribution networks.

4. Conclusions

The comprehensive study focused on the integration of a BESS into a real distribution network feeder with the aim of enhancing power quality and overall system efficiency. Through the simulation of various scenarios, both with and without photovoltaic generation (PVDG), the study revealed significant improvements in LF and PF resulting from the integration of the BESS. Notably, the LF showed an approximate increase of 21.05% without PVDG and 16.05% with 25% PVDG, showcasing the significant potential for improving the network's load management capabilities.

The BESS effectively maintained the PF above the critical threshold of 0.92 lagging in most scenarios, except in specific cases which constant reactive power injection was employed. Furthermore, the analysis of losses along the feeder indicated a slight reduction, emphasising the positive impact of the BESS integration on overall system efficiency. Although the current study did not explicitly delve into voltage impact assessments, observations suggested that potential voltage violations could be mitigated through transformer tap adjustments, highlighting the flexibility and adaptability of the system.

Future endeavours will focus on the optimisation of BESS placement to further reduce losses, explore advanced charging and discharging algorithms to improve efficiency, and investigate the feasibility of implementing BESS at distribution-level voltage levels with enhanced reactive power control. These initiatives aim to not only enhance power quality and reduce losses but also maximise the potential benefits of energy storage integration in complex distribution networks. The findings from this study emphasise the importance of strategic BESS integration and provide valuable insights for future sustainable and efficient distribution network designs.

Funding: This research received no external funding.

Author contributions: Conceptualisation, T.L.C. and V.T.C.; Methodology, T.L.C. and V.T.C.; Software, T.L.C.; Validation, T.L.C., V.T.C. and J.J.A.S.; Formal Analysis, T.L.C., V.T.C. and J.J.A.S.; Investigation, T.L.C.; Resources, T.L.C. and V.T.C.; Data Curation, T.L.C. and R.T.; Writing – Original Draft Preparation, T.L.C., J.J.A.S. and R.T.; Writing – Review & Editing, V.T.C and R.T.; Visualisation, V.T.C, J.J.A.S. and R.T.; Supervision, V.T.C.; Project Administration, T.L.C..

Disclosure statement: The authors declare no conflict of interest.

References

[1] Asif Raihan and Almagul Tuspekova. Dynamic impacts of economic growth, energy use, urbanization, tourism, agricultural value-added, and forested area on carbon dioxide emissions in brazil. *Journal of Environmental Studies and Sciences*, 12(4):794–814, Aug 2022.

[2] Natsawat Pompern, Suttichai Premrudeepreechacharn, Apirat Siritaratiwat, and Sirote Khunkitti. Optimal placement and capacity of battery energy storage system in distribution networks integrated with pv and evs using metaheuristic algorithms. *IEEE Access*, 11:68379–68394, 2023.

[3] Nadeeshani Jayasekara, Mohammad A. S. Masoum, and Peter J. Wolfs. Optimal operation of distributed energy storage systems to improve distribution network load and generation hosting capability. *IEEE Transactions on Sustainable Energy*, 7(1):250–261, Jan 2016.

[4] Shahab Karrari, Nicole Ludwig, Giovanni De Carne, and Mathias Noe. Sizing of hybrid energy storage systems using recurring daily patterns. *IEEE Transactions on Smart Grid*, 13(4):3290–3300, Jul 2022.

[5] Alberto Grimaldi, Francesco Demetrio Minuto, Alessandro Perol, Silvia Casagrande, and Andrea Lanzini. Ageing and energy performance analysis of a utility-scale lithium-ion battery for power grid applications through a data-driven empirical modelling approach. *Journal of Energy Storage*, 65:107232, Aug 2023.

[6] Daniel Augusto Cantane, Oswaldo Hideo Ando Junior, and Márcio Biehl Hamerschmidt. *Tecnologias de Armazenamento de Energia Aplicadas ao Setor Elétrico Brasileiro*. Scienza, 2020.

[7] Ricardo Aldabó LOPEZ. Qualidade na energia elétrica: Efeitos dos distúrbios, diagnósticos e soluções. *São Paulo: Artliber*, 2013.

[8] Ye Yang, Hui Li, Andreas Aichhorn, Jianping Zheng, and Michael Greenleaf. Sizing strategy of distributed battery storage system with high penetration of photovoltaic for voltage regulation and peak load shaving. *IEEE Transactions on Smart Grid*, 5(2):982–991, Mar 2014.

[9] Sayed Mir Shah Danish, Mikaeel Ahmadi, Mir Sayed Shah Danish, Paras Mandal, Atsushi Yona, and Tomonobu Senjyu. A coherent strategy for peak load shaving using energy storage systems. *Journal of Energy Storage*, 32:101823, Dec 2020.

[10] Yu Zheng, Junhua Zhao, Yue Song, Fengji Luo, Ke Meng, Jing Qiu, and David John Hill. Optimal operation of battery energy storage system considering distribution system uncertainty. *IEEE Transactions on Sustainable Energy*, 9(3):1051–1060, Jul 2018.

[11] Pei Yong, Ning Zhang, Qingchun Hou, Yuxiao Liu, Fei Teng, Song Ci, and Chongqing Kang. Evaluating the dispatchable capacity of base station backup batteries in distribution networks. *IEEE Transactions on Smart Grid*, 12(5):3966–3979, Sep 2021.

[12] Rafael Sebastián. Application of a battery energy storage for frequency regulation and peak shaving in a wind diesel power system. *IET Generation, Transmission Distribution*, 10(3):764–770, Feb 2016.

[13] Qifeng Li, Raja Ayyanar, and Vijay Vittal. Convex optimization for des planning and operation in radial distribution systems with high penetration of photovoltaic resources. *IEEE Transactions on Sustainable Energy*, 7(3):985–995, Jul 2016.

[14] Mohsen Kalantar-Neyestanaki and Rachid Cherkaoui. Coordinating distributed energy resources and utility-scale battery energy storage system for power flexibility provision under uncertainty. *IEEE Transactions on Sustainable Energy*, 12(4):1853–1863, Oct 2021.

[15] Agência Nacional de Energia Elétrica - ANEEL. Resolução homologatória nº 2.120, de 16 de agosto de 2016, 2016.

[16] John Jefferson Antunes Saldanha and Marcos Samuel Jansen. Impacto da geração distribuída em uma rede elétrica real da cidade de Jaraguá do Sul. In *2022 Anais do Seminário de Ensino, Pesquisa e Extensão (SEPETEC)*, 2022.

[17] Alexandre Klabunde and Vitor Teles Correia. Utilização do controle volt/var como alternativa para mitigar as transgressões de nível de tensão elétrica em um alimentador da rede de distribuição com alta penetração de energia fotovoltaica. *IFSC, Jaraguá do Sul*, 2022.

[18] Marcos Samuel Jansen and John Jefferson Antunes Saldanha. Análise do impacto da geração distribuída fotovoltaica em uma rede elétrica da cidade de Jaraguá do Sul. *IFSC, Jaraguá do Sul*, 2022.

[19] Paulo Ricardo Radatz de Freitas. Modelos avançados de análise de redes elétricas inteligentes utilizando o software OpenDSS. *USP, São Paulo*, 2015.

[20] EPRI. Storage element. Technical report, EPRI, 2020.

[21] EPRI. Storage controller element. Technical report, EPRI, 2020.

[22] WEG. ESSW sistema de armazenamento de energia em baterias, 2022.

[23] Keith Malmedal and P. K. Sen. A better understanding of load and loss factors. *2008 IEEE Industry Applications Society Annual Meeting*, Oct 2008.